RESEARCH ARTICLE

Human Mutation

OFFICIAL JOURNAL HGVS HUMAN GENOME VARIATION SOCIETY www.hgvs.org

Germline Chromothripsis Driven by L1-Mediated Retrotransposition and Alu/Alu Homologous Recombination

Lusine Nazaryan-Petersen,[1,2*] Birgitte Bertelsen,[1] Mads Bak,[3] Lars Jønson,[4] Niels Tommerup,[3] Dustin C Hancks,[5†] and Zeynep Tümer[1†]

[1]*Applied Human Molecular Genetics, Kennedy Center, Department of Clinical Genetics, Copenhagen University Hospital, Rigshospitalet, Glostrup 2600, Denmark;* [2]*Department of Cellular and Molecular Medicine (ICMM), Faculty of Health Science, University of Copenhagen, Copenhagen N. 2200, Denmark;* [3]*Department of Cellular and Molecular Medicine, Faculty of Health Science, University of Copenhagen, Copenhagen N. 2200, Denmark;* [4]*Center for Genomic Medicine, Copenhagen University Hospital, Rigshospitalet, Copenhagen O. 2100, Denmark;* [5]*Department of Human Genetics, University of Utah School of Medicine, Salt Lake City, Utah 84112*

Communicated by David N. Cooper

Received 10 November 2015; accepted revised manuscript 3 January 2016.
Published online 14 January 2016 in Wiley Online Library (www.wiley.com/humanmutation). DOI: 10.1002/humu.22953

ABSTRACT: **Chromothripsis (CTH) is a phenomenon where multiple localized double-stranded DNA breaks result in complex genomic rearrangements. Although the DNA-repair mechanisms involved in CTH have been described, the mechanisms driving the localized "shattering" process remain unclear. High-throughput sequence analysis of a familial germline CTH revealed an inserted SVA_E retrotransposon associated with a 110-kb deletion displaying hallmarks of L1-mediated retrotransposition. Our analysis suggests that the SVA_E insertion did not occur prior to or after, but concurrent with the CTH event. We also observed L1-endonuclease potential target sites in other breakpoints. In addition, we found four *Alu* elements flanking the 110-kb deletion and associated with an inversion. We suggest that chromatin looping mediated by homologous *Alu* elements may have brought distal DNA regions into close proximity facilitating DNA cleavage by catalytically active L1-endonuclease. Our data provide the first evidence that active and inactive human retrotransposons can serve as endogenous mutagens driving CTH in the germline.**

Hum Mutat 37:385–395, 2016. © 2016 Wiley Periodicals, Inc.

KEY WORDS: ***Alu*; chromothripsis; LINE-1; L1; nonallelic homologous recombination; NAHR; SINE-VNTR-Alu; SVA**

Introduction

Chromothripsis (CTH) was first characterized in cancer where hundreds of DNA double-strand breaks (DSBs) are localized in relatively small genomic regions ranging from a few hundred kb up to several Mb in size or in larger regions as whole chromosome arms or even entire chromosomes [Stephens et al., 2011; Kloosterman et al., 2011b]. The frequency of CTH is 2%–3% in many cancer forms and up to 25% in bone cancers [Stephens et al., 2011]. CTH has also been observed in benign tumors, but with significantly fewer breakpoints (BPs) [Mehine et al., 2014]. Subsequently, CTH was also detected in congenital and developmental disorders and was termed germline CTH (G-CTH) [Kloosterman et al., 2011a, 2012; Chiang et al., 2012; Nazaryan et al., 2014), but compared with various human cancers only a limited number of G-CTH cases have been described to date.

It has been hypothesized that CTH is initiated by extracellular or intracellular genotoxic factors (such as ionizing radiation and reactive oxygen substances) where the whole chromosome or part of it is shattered into multiple pieces generating clustered DSBs, which are subsequently "stitched" together in a random order [Stephens et al., 2011; Chiang et al., 2012; Kloosterman et al., 2012). In general, DSBs are repaired through different mechanisms such as homologous recombination [Li and Heyer, 2008), nonhomologous end-joining (NHEJ) [Lieber. 2010] or microhomology mediated end-joining (MMEJ) [McVey and Lee, 2008]. The BP junction (BPJ) sequence features of the hitherto described relatively balanced CTH cases suggest that the multiple DSBs are primarily joined together by NHEJ and MMEJ repair mechanisms [Chiang et al., 2012; Kloosterman et al., 2012). As a result, a patchwork of genomic fragments generates complex rearrangements involving translocations, inversions, and insertions. This mechanism may explain why CTH is relatively balanced, although deletions are occasionally observed [Kloosterman et al., 2012]. On the other hand, in chromoanasynthesis (a CTH-like phenomenon) replication based repair mechanisms, such as fork stalling and template switching (FoSTeS), and microhomology mediated break-induced replication, are thought to be involved, resulting in clustered duplications and triplications [Liu et al., 2011]. Recent single cell sequencing experiments have shown that CTH can occur subsequent to partition of an intact chromosome or part of a chromosome into a micronucleus [Zhang et al., 2015], as chromosomes in micronuclei are underreplicated and can accumulate DNA damages [Crasta et al., 2012]. However, in the relatively balanced CTH cases, it is still unclear which mechanism(s) drive the localized shattering process and whether additional repair machineries other than NHEJ and MMEJ might be implicated.

LINE-1 (L1) retrotransposons are endogenous mutagens that mobilize through an RNA intermediate via a copy-and-paste

Additional Supporting Information may be found in the online version of this article.

†These authors are cosenior authors.

*Correspondence to: Lusine Nazaryan-Petersen, Department of Cellular and Molecular Medicine (ICMM), Faculty of Health Science, University of Copenhagen, Copenhagen N. 2200, Denmark. E-mail: nlucine@sund.ku.dk

Contract grant sponsors: Lundbeck Foundation (grant numbers: R24-A2419, R100-A9332, R151-2013-14290, and R169-2014-2186); American Cancer Society (grant number: PF-13-371-01-MPC); University of Copenhagen.

mechanism [Kazazian, 2004]. In humans, L1 is the only active autonomous retrotransposon that is capable of mobilizing itself [Moran et al., 1996; Kazazian, 2004] and other retrotransposons such as *Alu* [Kajikawa and Okada, 2002; Dewannieux et al., 2003] and SINE-VNTR-Alu (SVA) elements [Ostertag et al., 2003; Wang et al., 2005; Hancks et al., 2011; Raiz et al., 2012]. L1s encode two open-reading frames (ORF), one of which (ORF2p) has both DNA endonuclease [Feng et al., 1996] and reverse-transcriptase [Mathias et al., 1991] activities. During retrotransposition, genomic DNA is cleaved by the endonuclease activity at its target site followed by reverse transcription primed by the liberated 3′-OH, a mechanism termed target-primed reverse transcription [Luan et al., 1993; Cost, 2002]. L1 activity has been described in early development [Garcia-Perez et al., 2007; van den Hurk et al., 2007; Kano et al., 2009] and in a variety of cancers [Lee et al., 2012a; Solyom et al., 2012; Helman et al., 2014; Shukla et al., 2014; Tubio et al., 2014]. It has also been shown that L1 and SVA elements are expressed in human germinal vesicles and that de novo retrotransposition events can occur in human primary oocytes [Georgiou et al., 2009]. Previous studies have shown a correlation between retrotransposon sequences and genomic structural variants [Deininger and Batzer, 1999; Batzer and Deininger, 2002; Sen et al., 2006; Lee et al., 2008] and segmental duplications [Bailey et al., 2003] in the human genome.

Here, we describe a SVA element retrotransposition event and *Alu* sequences associated with BPs in a G-CTH stably segregating through three generations. We suggest a model where chromatin looping of distal DNA regions mediated by homologous *Alu* elements poises DNA for CTH followed by DNA cleavage by the L1 endonuclease. This model can also explain the inverted orientation of the genomic fragments flanking the retrotransposed SVA element. Overall, this is the first report of active and inactive retrotransposons associated with CTH, suggesting that different repair mechanisms may cooperate depending on the specific sequence signatures of the broken DNA.

Materials and Methods

PCR Cloning of the BPJs and Sanger Sequencing

The rearrangements and the BPs involved in this G-CTH were initially identified with next-generation mate-pair sequencing in four members of a three generation family (accession numbers SRR1596548; SRR1611133; SRR1611136; and SRR1611134) (described in Bertelsen et al., 2015). To fine map these BPJs, sequences flanking the BP regions were obtained from the UCSC Human Genome Browser and masked for repetitive sequences using RepeatMasker, as previously described [Nazaryan et al., 2014]. Primers for each BPJ were designed using Primer3 [Untergrasser et al., 2012] and PCR was performed on genomic DNA from the family members I:1, II:2, II:4, II:6, III:2, III:14, III:15 (Supp. Fig. S1) and a normal control. Informed consents were obtained from all subjects. Amplified BP-spanning fragments were sequenced using BigDye-terminator chemistry and an ABI 3130XL genetic analyzer (ABI, Columbia, MD). Obtained sequences were aligned to the human reference genome (*hg19*) and BPs were determined using the EMBOSS Needle nucleotide alignment tool (http://www.ebi.ac.uk/Tools/psa/emboss_needle/nucleotide.html). Sequences spanning the BPJs obtained from Sanger sequencing have been submitted to the GenBank with the accession numbers KP083371-KP083409 (Supp. Table S1).

Examination of the BPs and BPJs for Underlying Mechanisms

Indels (small deletions and insertions) at the BP regions were visualized by splitting the BPJ sequences at the BPs and aligning them to genomic DNA of the BP region. BPJs were also examined for microhomology and for the presence of any repetitive elements to evaluate the putative repair mechanisms involved during the G-CTH process. The inserted SVA_E sequence was compared with the datasets of the polymorphic human retrotransposon insertions through targeted [Beck et al., 2010; Ewing and Kazazian, 2010; Huang et al., 2010; Iskow et al., 2010; Witherspoon et al., 2010] or whole-genome resequencing [Ewing and Kazazian, 2011; Stewart et al., 2011]. The 5′- and 3′-BPJs flanking the SVA_{CTH} sequence were examined with regard to the target-site duplications. All the BPs were screened for L1 endonuclease cleavage sites (5′-YYYY/RR-3′) [Feng et al., 1996; Ostertag et al., 2003). The SVA_{CTH} sequence has been submitted to GenBank with the accession number KP162058.

Results

In this study, we analyzed the BPJ sequences of a G-CTH involving chromosomes 3 and 5 (Fig. 1A and B) identified in 11 members of a three generation family (Supp. Fig. S1). The BPJs were identified by next-generation mate-pair sequencing and chromosome microarray analysis (described in Bertelsen et al., 2015). The rearrangements were validated by PCR and Sanger sequencing of DNA from seven family members representing all the three generations. These data enabled fine mapping of the six BPJs to single base pair level (Fig. 2; Supp. Table S1). All the BPJ sequences were identical in all investigated G-CTH carriers; thus, the G-CTH segregated stably through three generations.

Complex Rearrangements and BPJs

On chromosome 5, there was a single BP, whereas at 3q22.3-q23 an approximately 6.4 Mb region was shattered by six DNA breaks generating seven fragments (3a–3g), where the ∼110 kb fragment 3c was deleted (Fig. 1A). Furthermore, Sanger sequencing revealed small deletions ranging from 2 to 70 bp at three BPs (3a/3b; 3d/3e; and 5a/5b; Fig. 1A), two microhomologies at BPJ-3a_3e and BPJ-3b_5b, and a 177-bp homology at BPJ-3e_3f due to the presence of flanking *Alu* elements (Fig. 2A, B, and D). Finally, a 5′-truncated SVA_E element insertion (502 bp) was observed at BPJ-3d_3g (Fig. 2F).

CTH Rearrangements Were Associated with *Alu*/*Alu* Nonallelic Homologous Recombination

We identified *Alu* elements at four of the seven BP-sequences (3b/3c, 3c/3d, 3d/3e, 3e/3f; Figs. 1A and 3A). *Alu* elements are ∼300 bp primate-specific SINE retrotransposons [Ade et al., 2013] and due to their high copy number (∼1 million copies in the human genome), these elements are prone to NAHR events. Such events have resulted in benign and pathogenic genomic deletions, duplications, and inversions in humans [Deininger and Batzer, 1999; Batzer and Deininger, 2002; Sen et al., 2006; Lee et al., 2008].

Two *AluSx* elements flanking the 110-kb deleted 3c-fragment are in the same orientation: one located 27 bp upstream of the BP-3b/3c and the second spanning the BP-3c/3d (Fig. 3A). Several reports have described intra- and interchromosomal *Alu* sequences in the same orientation resulting in gross deletions (reviewed in Deininger and

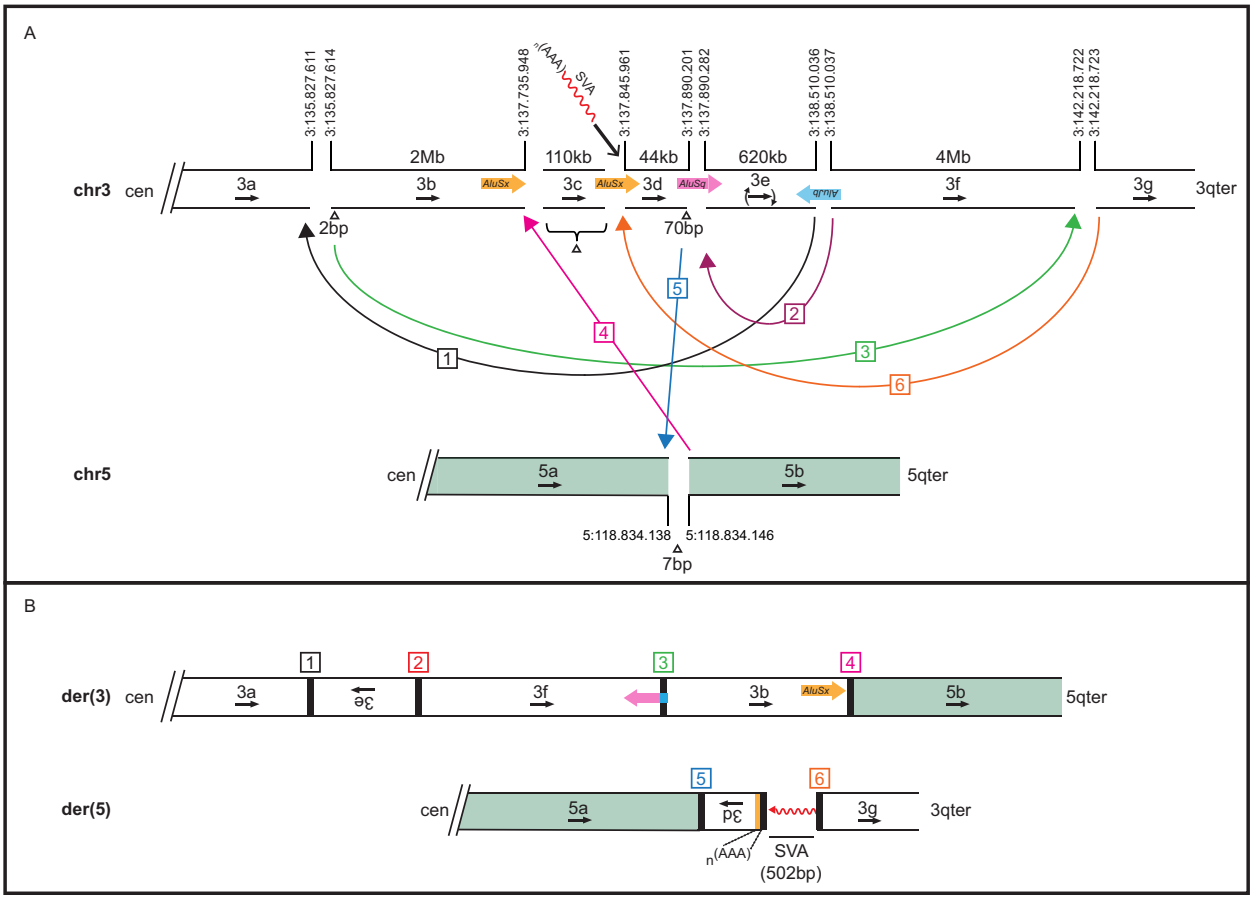

Figure 1. Heritable germline chromothripsis. **A**: Diagram of the reference chromosomes (chr) 3 and 5 prior to chromothripsis. Fragments involved in the chromothriptic rearrangement are labeled 3a–3f and 5a–5b. Sizes of internal fragments are indicated above each corresponding DNA fragment. Rearrangements are highlighted by colored arrows between putative breakpoints. A red curvy line indicates the SVA RNA and the site of retrotransposition at breakpoint 3c/3d. Δ denotes sites where genomic sequence was deleted during chromothripsis. Black arrows below fragment names indicate orientation of genomic fragments. Alu elements implicated in chromothripsis are shown. Genomic coordinates at breakpoints are according to *hg19*. **B**: Diagram of derived chromosomes 3 and 5 following chromothripsis as determined by next-generation mate-pair sequencing and breakpoint junction resequencing. Mb, megabase; kb, kilobase; bp, basepair; cen, centromere; SVA, SINE VNTR Alu retrotransposon; BP, breakpoint.

Batzer, 1999). This deletion also results in the truncation of the *AluSx* element, where only a 21-bp polyA stretch of the *AluSx*, representing the 5′-end of fragment 3d, remains at the site of the SVA integration (Figs. 1B and 2F).

Two other *Alu* elements spanning the BPs of the fragment 3e prior to the inversion are from different subfamilies (*AluSq* at the BP 3d/3e and *AluJb* at the BP 3e/3f) and in opposite orientations (Fig. 1A). The 5′-end of the *AluSq* was translocated to chromosome 5 (Fig. 1B) and processed further by DNA repair resulting in a 70-bp deletion, a 9-bp inversion, and a 5-bp inversion-duplication (invdup) within the *AluSq* sequence at the final BPJ-5a_3d (Fig. 2E). Following the CTH event, the 3′-end of *AluSq* was attached to the 5′-end of *AluJb* resulting in the formation of a chimeric *Alu* element at the BPJ-3e_3f (Figs. 1B and 2B). Chimeric Alu elements are often observed at Alu-associated inversions [Lee et al., 2008].

LINE-1-Mediated Retrotransposition of an SVA Element at the BPJ 3d_3g

The 502-bp SVA_E element (hereafter referred to as SVA_{CTH}) inserted into intron 2 of *A4GNT* (alpha-1,4-N-acetylglucosaminyltransferase) is associated with the occurrence of ~110 kb deletion (fragment 3c) located at the 5′-end (Fig. 1A). However, the inserted SVA_{CTH} did not connect the fragments 3b and 3d together but appeared in between the BPJ-3d_3g (Fig. 2F). SVA elements are hominid-specific nonautonomous retrotransposons mobilized by L1 in *trans* [Ostertag et al., 2003; Wang et al., 2005; Hancks et al., 2011; Raiz et al., 2012]. To investigate whether this insertion was a result of an L1-mediated retrotransposition or a NAHR event, a known mechanism by which retrotransposons can lead to deletions, we examined the 5′- and 3′-BPJs flanking the SVA_{CTH} sequence in more detail. Our analysis revealed that SVA_{CTH} displays characteristics of L1-mediated retrotransposition. Specifically, the 5′-end of SVA_{CTH} is truncated (at the very 3′-end of the SVA VNTR domain) and the insertion occurred within a sequence resembling the L1 endonuclease cleavage site (5′-TTTT/GA-3′) [Feng et al., 1996; Ostertag et al., 2003], where a single nucleotide (T) is deleted at the 3′-end of the insertion (Fig. 2F).

L1-mediated insertions, including *Alu* and SVA retrotransposons, associated with large genomic deletions have been identified previously [Gilbert et al., 2002; Symer et al., 2002; Callinan et al., 2005; Chen et al., 2005; Gilbert et al., 2005; Han et al., 2005; Hancks and Kazazian, 2012; Lee et al., 2012b]. To determine whether the current

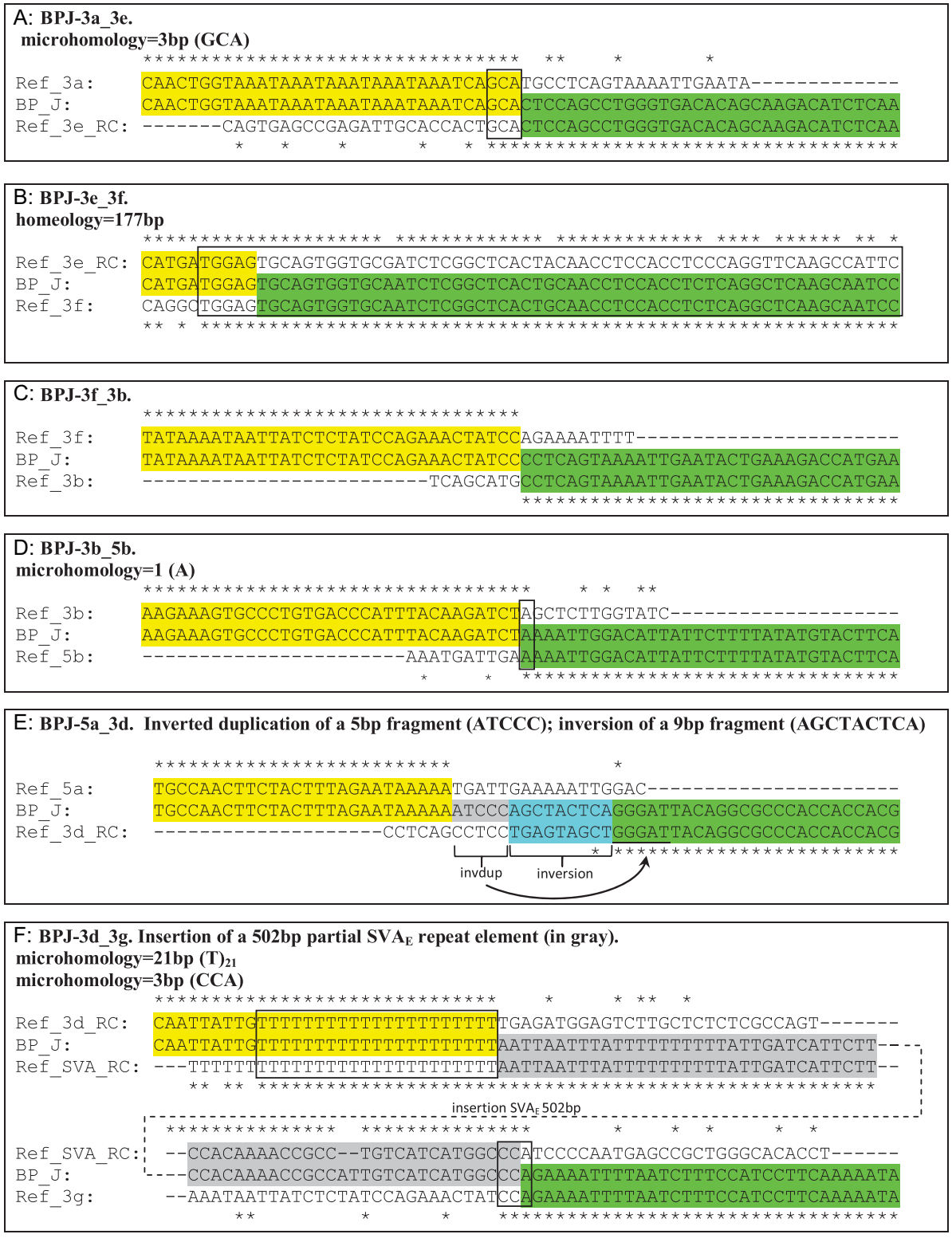

Figure 2. Sequence features of the breakpoint junctions (BPJs). The sequence features of the six BPJs are shown in separate boxes. The names of the BPJs correspond to those in Figure 1B (e.g., 3a_3e, 3e_3f). The breakpoint sequences prior to chromothripsis (yellow and green) aligned to the reference sequences of the corresponding joined fragments are shown (e.g., Ref_3a and Ref_3e_RC). Whenever it was necessary, the sequences were reverse complemented (RC). Microhomology is outlined by black frames. Other variations (insertions, duplications, and inversions) at the BPJs are indicated separately. Asterisks indicate homology between two sequences.

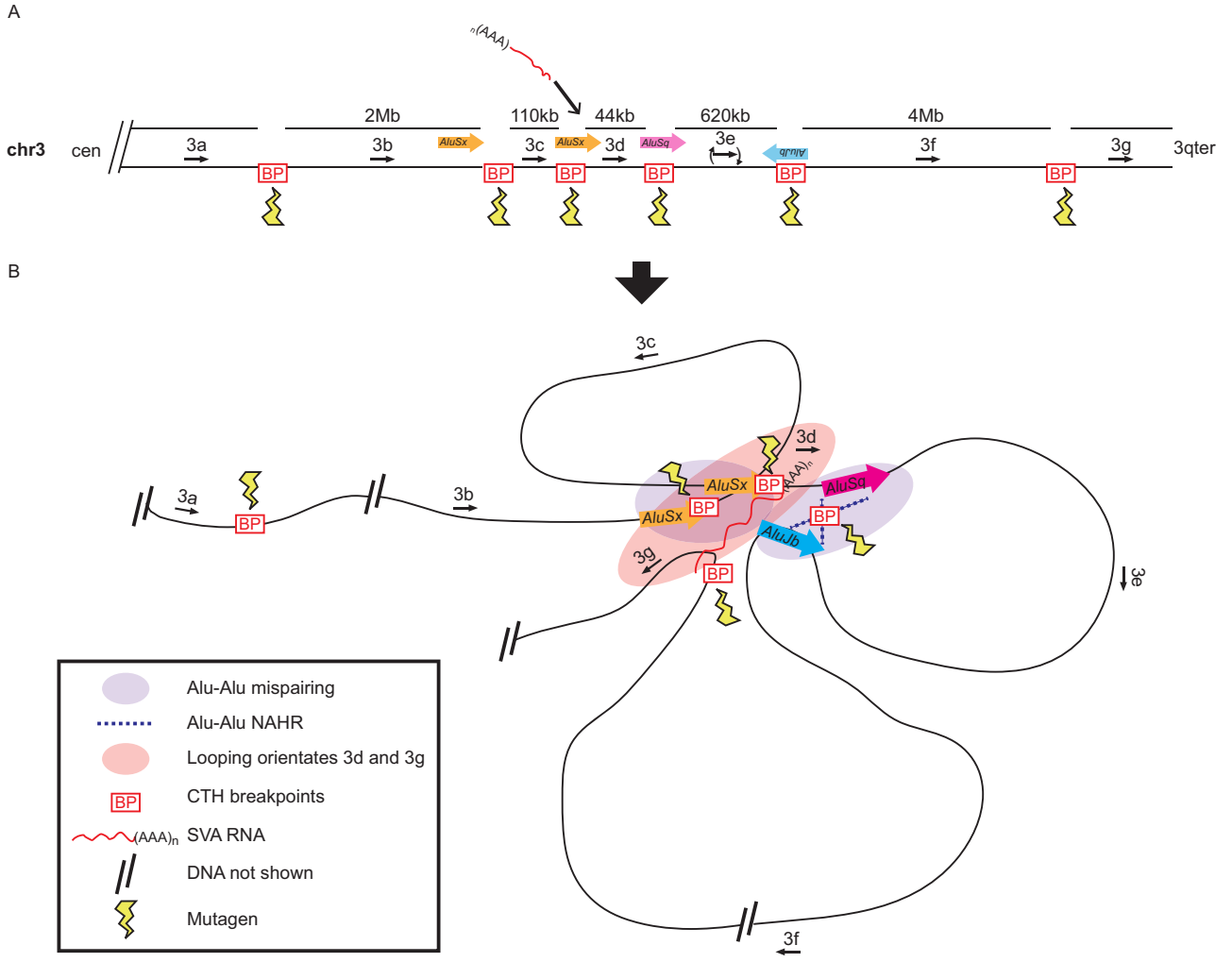

Figure 3. Chromatin looping mediated by nonallelic genomic Alus poised configuration of reference chromosomes prior to chromothripsis. **A**: Chromosome 3 configuration prior to chromothripsis. Labeling is identical to Figure 1. Yellow lightning bolts indicate putative mutagen driving shattering of chromosome 3. **B**: Diagram of chromatin looping model prior to chromothripsis involving chromosome 3. Alu elements implicated in chromothripsis are shown. Mispairing of two nonallelic *AluSx*s (orange arrows) in the same orientation flanking fragment 3c poise this locus for deletion. Mispairing of two nonallelic *Alu* elements (*AluSq* and *Alu Jb*) in opposite orientation results in the inversion of fragment 3e. Finally, additional looping organizes fragments 3d and 3g in opposite orientation accounting for the genomic flanking sequence configuration following SVA retrotransposition. A red curvy line indicates the SVA RNA and the site of retrotransposition.

SVA_{CTH} insertion resembled other human retrotransposition-associated deletions, we examined previously reported disease-causing insertions since they represent recent events where the original BPJs are likely intact (Table 1). Of the 104 disease-causing L1-mediated retrotransposition events reported to date, 20 were associated with deletions at the site of insertion with 17 of these deletions ranging from 1.4 kb to 1 Mb in size [Hancks and Kazazian, 2012; Vogt et al., 2014]. Notably, the retrotransposon insertions associated with large deletions display four characteristics that are shared with SVA_{CTH} (Table 1): (1) insertions occur at L1 endonuclease cleavage sites; (2) the 5′-ends of almost all insertions (15/17) are extremely truncated, some having only poly-A tails remaining; (3) the large deletion always occurs at the 5′-end of the insertion; and (4) all lack target-site duplications. In addition, we identified microhomology (5′-TGG-3′) between the 5′-end of SVA_{CTH} and the site of attachment at fragment 3g (Fig. 2F). Microhomology with the 5′-genomic flanking sequence is well documented for 5′-truncated L1-mediated insertions [Zingler et al., 2005]. Lastly, if SVA_{CTH} was a bona fide retrotransposition event, one would expect SVA_{CTH} to be derived from a full-length SVA source element. Indeed, BLAT search [Kent, 2002] shows that the 502-bp SVA_{CTH} shares 100% nucleotide identity to a full-length SVA located on chr7:1,185,078–1,187,654 (GRCh37) belonging to a known active subfamily (SVA_E) (Fig. 4F). Thus, SVA_{CTH} displays hallmarks of L1-mediated retrotransposition.

SVA_{CTH} Insertion Occurred During CTH

Next, we wanted to examine whether the SVA_{CTH} insertion occurred concomitantly with the G-CTH rearrangements. Three potential possibilities for the timing of the SVA_{CTH} insertion at the BPJ-3d_3g are: (1) SVA_{CTH} was inserted prior to the CTH event and thus may be polymorphic in the human population (SVA_{CTH} first); (2) SVA_{CTH} retrotransposed after the CTH rearrangements within this family (CTH first); or (3) SVA_{CTH} retrotransposed concurrently with the CTH event.

Table 1. Recent Retrotransposition-Associated Deletions in Humans

	Insertion	Gene	CHR	Reference	Disease	Subfamily	Size (bp)	polyA tail (bp)	Truncation	Transduction (bp)	Strand	Deletion	Target-site duplication (TSD)	L1 endo site (5′-TTTT/AA-3′)
1	Alu	*ABCD1*	X	Kutsche et al. (2002)	Adrenoleukodystrophy	AluYb9	98	20	Y/5′TR	N	S	4.7 kb	No TSD	ATTT/GT
2	Alu	*FVIII*	X	Sukarova et al. (2001)	Hemophilia A	AluYb8	290	47	FL	N	AS	3 nt	No TSD	TTTC/AT
3	Alu	*CTRC*	1	Masson et al. (2013)	Chronic pancreatitis	Alu	31	11	Y/5′TR	N	AS	53.9 kb	No TSD	TCTT/AT
4	Alu	*SERPINC1*	1	Beauchamp et al. (2000)	Type 1 antithrombin deficiency	Alu	6	40	Y/5′TR	N	AS	1.4 kb	No TSD	TTCT/AT
5	Alu	*APC*	5	Su et al. (2000)	Familial adenomatous polyposis	AluYb9	93	60	Y/5′TR	N	AS	1.6 kb	No TSD	TTTT/AA
6	Alu	*LPL*	8	Okubo et al. (2007)	Lipoprotein lipase deficiency	AluYb9	150	60	Y/5′TR	N	AS	2.2 kb	No TSD	TTTT/AA
7	Alu	*CHD7*	8	Udaka et al. (2007)	CHARGE syndrome	AluYa5/8	75	100	Y/5′TR	N	S	10 kb	No TSD	ATTT/AA
8	Alu	*PMM2*	16	Schollen et al. (2007)	Congenital disorders of glycosylation type Ia	AluYb8	263	10	Y/5′TR	N	AS	28 kb	No TSD	TTTT/AA
9	Alu	*BRCA1*	17	Peixoto et al. (2013)	Breast and ovarian cancer family	AluYc	191	60	Y/5′TR	N	AS	23.3 kb	No TSD	CTTT/AG
10	L1	*DMD*	X	Narita et al. (1993)	Duchenne muscular dystrophy	L1 Ta	608	16	Y/5′TR	N	AS	2 nt	No TSD	TCTT/AA
11	L1	*EYA1*	8	Morisada et al. (2010)	Branchio-oto-renal syndrome	L1 Hs	3,756	None	Y/3′TR	N	AS	17 kb	No TSD	TCTC/AG
12	L1	*FKTN*	9	Kondo-Iida et al. (1999)	Fukuyama-type congenital muscular dystrophy	L1Ta	1,200	59	Y/5′TR	N	S	6 nt	No TSD	TTTT/AA
13	L1	*PDHX*	11	Miné et al. (2007)	Pyruvate dehydrogenase complex deficiency	L1 Hs	6,086	67	FL	N	S	46 kb	No TSD	TTTT/AT
14	SVA	*A4GNT*	3	Nazaryan-Petersen et al. (current study)	Chromothripsis	E	502	None	Y/5′TR (VNTR)	N	AS	110 kb	No TSD	TTTT/GA
15	SVA	*HLA-A*	6	Takasu et al. (2007)	Leukemia	F_1	2,000	45	FL	N/A	AS	14 kb	No TSD	CCTT/AG
16	SVA	*SUZ1P*	17	Vogt et al. (2014)	Neurofibromatosis type I	F_1	1,700	23	Y/5′TR (VNTR)	Y (282/160)	AS	1 MB	No TSD	TTTT/AC
17	SVA	*SUZ1P*	17	Vogt et al. (2014)	Neurofibromatosis type I	F	1,300	40	Y/5′TR (VNTR)	No	AS	867 kb	No TSD	CTTT/AC
18	pA	*COL4A6*	X	Segal et al. (1999)	Alport syndrome	N/A	N/A	70	N/A	N/A	AS	13.4 kb	No TSD	TTCT/AT
19	pA	*AGA*	4	Jalanko et al. (1995)	Aspartylglucosaminuria	N/A	N/A	37	N/A	N/A	AS	2 kb	No TSD	TTCT/AA
20	pA	*BRCA2*	13	Wang et al. (2001)	Breast cancer	N/A	N/A	35	N/A	N/A	S	6.2 kb	No TSD	TTCT/AA

AS, antisense orientation relative to gene; bp, basepair; CHR, chromosome; endo, endonuclease; FL, full length; kb, kilobase; pA, polyA tail; S, sense orientation relative to gene; SVA, SINE VNTR Alu; TR, truncation; VNTR, variable number of tandem repeats.
Data for this table were compiled from the primary references listed. Reviewed in Hancks and Kazazian (2012).

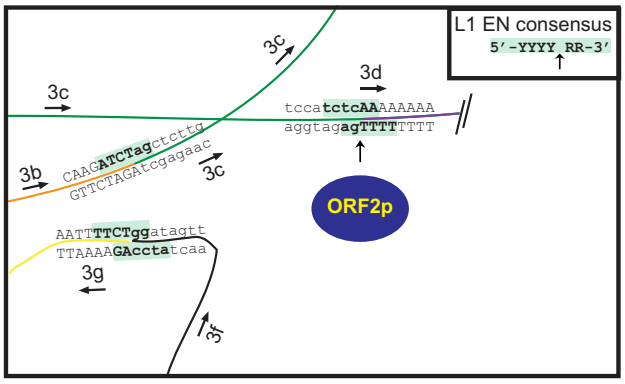

A: L1 ORF2p EN cleaves bottom strand (5′-TTTT/ga-3′)

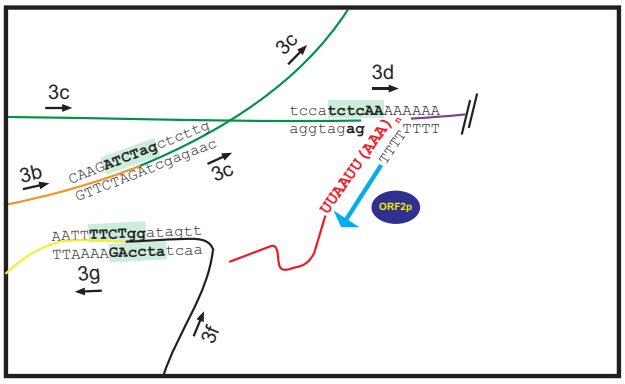

B: L1 ORF2p Reverse Transcription

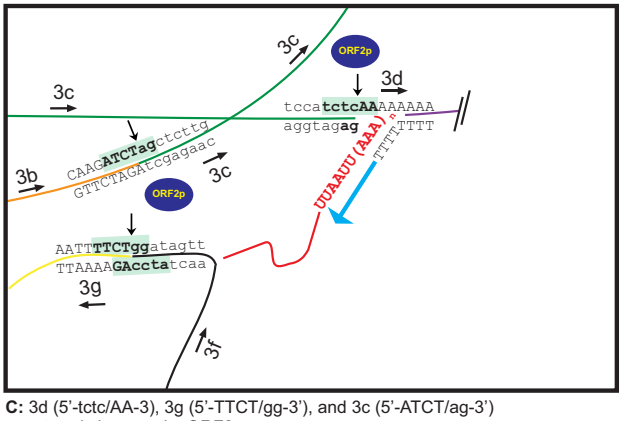

C: 3d (5′-tctc/AA-3), 3g (5′-TTCT/gg-3′), and 3c (5′-ATCT/ag-3′) top-strand cleavage by ORF2p

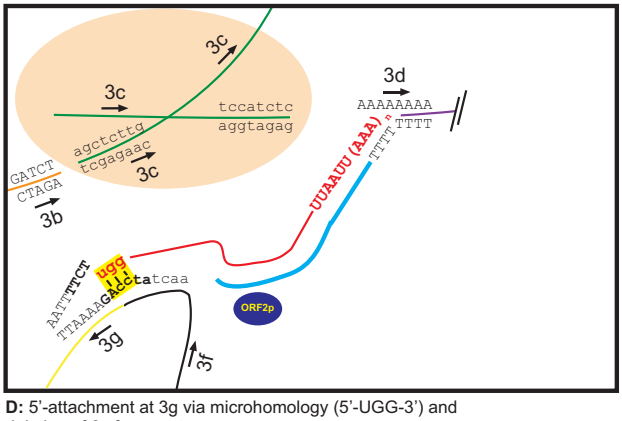

D: 5′-attachment at 3g via microhomology (5′-UGG-3′) and deletion of 3c fragment

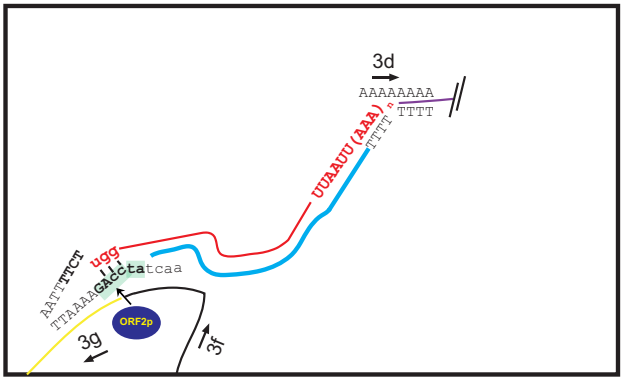

E: 3g bottom strand cleavage (5′-atcc/AG-3′) by ORF2p

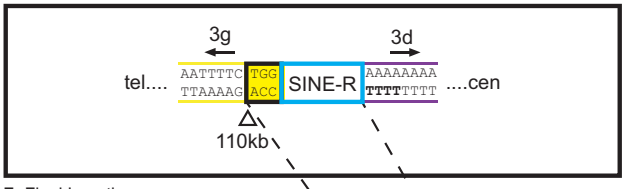

F: Final Insertion

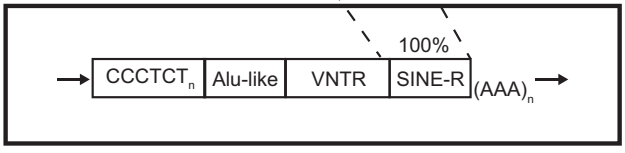

G: Potential Source Element (chr7:1,185,078-1,187,654)

Figure 4. L1-mediated retrotransposition of an SVA RNA drives DNA breakage resulting in chromosome 3 "shattering." An enhanced view of chromatin looping of chromosome 3 mediated by local *Alu* elements. Chromosome fragment orientation is similar to Figure 3. In addition, the naming and labeling of fragments involved in chromothripsis are similar to those in Figures 1 and 3; fragments are distinguished by colored lines. **A**: LINE-1 ORF2p cleaves (vertical black arrow) its target site on the bottom strand at the 3′-end of the *AluSx*. Breakpoint sequences implicated in establishing the final SVA insertion are shown. Sequence motifs similar to the L1 endonuclease consensus cleavage site are highlighted in green and bold text. SVA RNA not shown for clarity. Y, pyrimidine; R, purine. **B**: Following ORF2p cleavage of the bottom strand at the 3c/3d breakpoint, internal priming by ORF2p generates the first strand of cDNA (light blue line with arrowhead). A red curvy line indicates the SVA RNA and the site of retrotransposition. **C**: ORF2p endonuclease activity cleaves the top strand of 3b/3c and 3c/3d poising the 110-kb 3c fragment for deletion. Top-strand cleavage at 3g/3f by ORF2p liberates the DNA for infiltration by the 5′-end of the SVA RNA. Bottom-strand cleavage of the 3b/3c (not shown) may have been mediated by L1 endonuclease activity or nonspecific nuclease activity associated with the L1 RNA. **D**: Base-pairing interactions via microhomology (yellow) between 3g and the SVA RNA mediate 5′-attachment. **E**: ORF2p bottom-strand cleavage at 3g/3f initializes the resolution of the breakpoint at the 5′-end of the SVA insertion. **F**: Diagram of the final 5′-truncated SVA insertion located between the 3g and 3d breakpoints on the derived chromosome. Δ indicates the location of the 110-kb deletion of the 3c fragment at the 5′-end of the SVA insertion. SINE-R indicates the SVA domain that remains in the truncated insertion. **G**: Consistent with SVA_{CTH} being a retrotransposition event, a full-length SVA element belonging to a retrotranspositionally active SVA subfamily that shares 100% nucleotide sequence identity with the SVA_{CTH} insertion event was identified on chromosome 7 by BLAT analysis. The arrows indicate 5′-3′ orientation. Genomic coordinates are given according to *hg19*.

To investigate the "SVA_{CTH} first" hypothesis, we took advantage of recent studies that have identified tens of thousands of polymorphic human retrotransposon insertions through targeted [Beck et al., 2010; Ewing and Kazazian, 2010; Huang et al., 2010; Iskow et al., 2010; Witherspoon et al., 2010] or whole-genome resequencing [Ewing and Kazazian, 2011; Stewart et al., 2011]. By exploring this catalog, we did not identify the SVA_{CTH} insertion. Interestingly, we did find a polymorphic SVA_E insertion in the A4GNT gene in two datasets [Helman et al., 2014; Shukla et al., 2014; Adam D. Ewing, personal communication]. However, analysis of the target-site duplication and L1 endonuclease site for this polymorphic SVA confirmed that it was a distinct insertion, albeit on the same strand 591 bp upstream of the current SVA_{CTH}.

Regarding the "CTH first" hypothesis, none of the G-CTH events observed in this family over three generations lacked the SVA_{CTH} insertion, suggesting that the SVA_{CTH} was associated with the CTH event. This observation argues against the "CTH first" hypothesis, but as we do not know whether the G-CTH occurred de novo in the first generation of this family, we cannot exclude that the previous generation might have had the G-CTH without the presence of SVA_{CTH}.

In addition, an argument against both "SVA_{CTH} first" and "CTH first" models is that the SVA_{CTH} insertion region is within the 6.4-Mb shattered region on chromosome 3 and thus located near the flanking chromothriptic BPs (110 and 44 kb for upstream and downstream BPs, respectively), which is very unlikely to happen by chance since de novo SVA retrotranspositions are very rare events (one in 916 births; Xing et al., 2009). Lastly, the other counterparts of the BPs where the SVA_{CTH} insertion was observed, are involved in other chromothriptic rearrangements (BPJs-3f_3b and BPJ-3b_5b), which contradicts both "SVA_{CTH} first" and "CTH first" models. Combined, these observations favor the hypothesis that SVA_{CTH} insertion occurred concurrently with the other chromothriptic rearrangements within one cell cycle.

Discussion

CTH is considered to be a complex genomic rearrangement where multiple clustered BPs resemble a local shattering of genomic regions by unknown mutagen factors [Stephens et al., 2011]. Until now, the main suggested mechanisms for DSB repair in relatively balanced CTH cases are NHEJ and MMEJ [Stephens et al., 2011; Chiang et al., 2012; Kloosterman et al., 2012], whereas NAHR has been rather excluded [Malhotra et al., 2013]. In this study, through analysis of BPJ sequences of a familial G-CTH, we identified *Alu* elements and an evidence for L1-mediated retrotransposition at the BPs, which are implicated in the formation of this G-CTH rearrangements.

Several sequence features involved in this familial G-CTH implicate specific DNA repair mechanisms: first, the sequence features of the BPJs-3f_3b and BPJ-5a_3d (no homology, short deletions, insertions, and inversions; Fig. 2C and E) suggest usage of the NHEJ repair mechanism, which relies on the activities of the Ku70/80 heterodimer and the DNA ligase IV/XRCC4 complex [Lieber, 2010]. Second, we detected two very short microhomologies, GCA and A at the BPJs-3a_3e and BPJ-3b_5b, respectively (Fig. 2A and D), indicating that these BPJs might be repaired in a Ku70/80 and DNA ligase IV independent manner by the MMEJ repair machinery [McVey and Lee, 2008]. Thus, four out of six BPJs of the present G-CTH display footprints of NHEJ and/or MMEJ, which is consistent with previous reports [Chiang et al., 2012; Kloosterman et al., 2012]. However, the remaining two BPJs harbor different sequence hallmarks (177 bp homeology and inserted retrotransposon, respectively), not previously reported in CTH.

Based upon numerous reports of *Alu* element-associated genetic instability, we hypothesize that the *Alu* elements residing at four BPs (3b/3c, 3c/3d, 3d/3e, and 3e/3f; Fig. 3A) may have triggered the formation of two large hairpin loops and facilitated physical interactions between distally located DNA regions (Fig. 3B). The presence of inverted *Alu* elements (*AluSq* and *AluJb*) flanking the BPJ-3e_3f (Fig. 2B) supports the involvement of *Alu*/*Alu* recombination-mediated DSB repair (Fig. 3B), a mechanism that has previously only been shown in two-way rearrangements [Elliott et al., 2005]. Isolated *Alu*/*Alu* NAHR events between oppositely orientated *Alu* elements resulting in genomic inversions are well-documented [Li and Bray, 1993; Lee et al., 2008]. Therefore, these data suggest that different repair machineries may cooperate in G-CTH formation, depending on the genomic context of the broken DNA.

LINE-1 Activity Contributes to CTH

In this study, we report the first retrotransposition event occurring in association with G-CTH. Our data implicate involvement of L1 endonuclease activity leading to several DNA breaks and mediating SVA_{CTH} retrotransposition associated with a deletion, the model of which is outlined in Figure 4. The first likely step was the cleavage of the target sequence (5′-TTTT/GA-3′) at the BP-3c/3d by the ORF2p endonuclease (Fig. 4A). The SVA_{CTH} insertion indicates that ORF2p had initiated reverse-transcription directly upstream of the SVA mRNA polyA tail (Fig. 4B). This is evidenced by the lack of a distinct SVA_{CTH} polyA tail at the insertion site and the remnants of the *AluSx* polyA tail at the target site. Reverse-transcription upstream (5′-) of the polyA tail has previously been observed for L1-mediated insertions [Ovchinnikov et al., 2001; Callinan et al., 2005; Srikanta et al., 2009; Morisada et al., 2010), and this phenomenon is referred to as "internal priming." In addition, short polyA tails have been associated with L1 retrotransposition-mediated deletions in vivo (Table 1).

The next step was presumably the cleavage of the second strand (top-strand). Although the timing of this cleavage relative to the bottom-strand cleavage at BP-3c/3d is uncertain, it is generally hypothesized that this event follows the first cleavage event [Christensen and Eickbush, 2005]. In this instance, multiple DNA breaks mediated by ORF2p endonuclease activity may have driven the loss of the 3c fragment and have facilitated 5′-attachment of the SVA RNA (Fig. 4C). In addition to a strong L1 endonuclease site (5′-TCTC/AA-3′) directly above the bottom strand nick, other sequence motifs resembling the L1 endonuclease consensus site (5′-YYYY/RR, where Y = pyrimidine, R = purine) are located on the top strand of BP-3b/3c (5′-ATCT/AG-3′) and on the top and bottom strands of BP-3g/3f (5′-TTCT/GG-3′ and 5′-ATCC/AG-3′) (Fig. 4C). L1 endonuclease top-strand cleavage directly above bottom-strand cleavage is hypothesized to have occurred in the instances where small deletions have been observed with pathogenic insertions (Table 1).

One possibility for the dissociation and complete loss of the 3c fragment would be NAHR due to the presence of two homologous *AluSx* elements flanking this segment in the same orientation (Fig. 1A). However, in case of a classical NAHR involving DNA replication, which would result in deletion of the 3c fragment, one would expect ligation of the 3b fragment to 3d. Notably, the 3b and 3d fragments are not ligated and have different counterparts (5b and 3g fragments, respectively) (Fig. 1B). The second hypothesis for the deletion of the 3c fragment requires the presence of two DSBs (BP-3b/3c and BP-3c/3d). We speculate that although the BP-3b/3c is linearly distal to BP-3c/3d, chromatin looping mediated by homologous *AluSx* elements may have brought this DNA fragment

in close proximity with catalytically active ORF2p positioned near the BP-3c/3d leading to DNA cleavage (Fig. 3B). Consistent with this model, overexpression of L1 ORF2p has been associated with widespread DSBs in vivo [Gasior et al., 2006] and an additional nuclease activity has been associated with ORF2p in vitro that differs from the canonical L1 endonuclease activity [Cost, 2002; Kopera et al., 2011].

A DNA break of at least one strand, potentially by the L1 endonuclease, at BP-3f_3g (Fig. 4C) has likely enabled invasion of the SVA_{CTH} RNA. Following this event, consistent with the presence of microhomology between 3g and the SVA RNA (5′-TGG-3′), we posit that the 5′-end of the SVA_{CTH} RNA basepaired with 3g DNA. This suggestion is supported by the knowledge that microhomologies are common at the 5′-ends of L1-mediated insertions and are hypothesized to be the primary means of 5′-attachment of non-LTR retrotransposon sequences [Gilbert et al., 2002; Symer et al., 2002; Gilbert et al., 2005). Most of the L1 5′-attachment models propose that 5′-attachment occurs via base pairing interactions between the newly synthesized cDNA and the upstream flanking sequence following top-strand cleavage [Gilbert et al., 2002; Symer et al., 2002; Gilbert et al., 2005; Zingler, 2005; Babushok et al., 2006). However, we suggest that, at least in this instance, 5′-attachment may have been mediated by base pairing between microhomologies of the SVA_{CTH} RNA and BP-3f/3g.

Overall, it is difficult to speculate the steps following 5′-attachment, as these are generally poorly understood for human retrotransposons. Basepairing of the SVA_{CTH} RNA instead of the first-strand SVA_{CTH} cDNA may account for the 5′-truncation. Here, during reverse transcription, the SVA_{CTH} RNA and ORF2p would collide with the BP-3f/3g leading to disengagement of ORF2p from its RNA template. Next, top-strand SVA_{CTH} cDNA synthesis may have occurred followed by DNA repair. Furthermore, chromatin looping might explain the inverted orientation of the 3g fragment relative to the 3d fragment (Fig. 3B) following SVA_{CTH} retrotransposition (Figs. 1B and 4F). Therefore, this model can account for the BP 3′- of SVA_{CTH}, the 110-kb deletion of the 3c fragment, the BP 5′- of SVA_{CTH}, and the 5′-attachment of the SVA_{CTH} element.

In conclusion, these data uncover and suggest an association of active and inactive retrotransposons at CTH BPs. L1 activity has been described at the time point when CTH is believed to take place. This, taken together with the abundance of genomic LINEs and SINEs, the fact that their polyA tails (bottom strand) resemble the L1 endonuclease cleavage site (i.e., BP-3c/3d), coupled with the evidence that numerous genomic L1-mediated insertions nest within each other, may in part explain the "mystery" of the clustered BPs observed in CTH. Further studies of other BPJs involved in CTH cases will be necessary to elucidate the role of these endogenous mutagens in CTH formation.

Acknowledgments

We thank Haig H. Kazazian Jr. for initial consultation on the project.

L.N.-P. and N.T. conceived the hypothesis, and D.C.H. developed the model. L.N.-P. and D.C.H. wrote the paper, Z.T. made the final review, and all the authors discussed the results and commented on the manuscript and gave their final approval. L.N.-P., B.B., and L.J. performed experimental procedures. L.N.-P., M.B., and D.C.H. performed data analysis. Z.T. led the project.

Disclosure statement: The authors have no conflicts of interest to declare.

References

Ade C, Roy-Engel AM, Deininger PL. 2013. Alu elements: an intrinsic source of human genome instability. Curr Opin Virol 3:639–645.

Babushok DV, Ostertag EM, Courtney CE, Choi JM, Kazazian HH. 2006. L1 integration in a transgenic mouse model. Genome Res 16:240–250.

Bailey JA, Liu G, Eichler EE. 2003. An Alu transposition model for the origin and expansion of human segmental duplications. Am J Hum Genet 73:823–834.

Batzer MA, Deininger PL. 2002. Alu repeats and human genomic diversity. Nat Rev Genet 3:370–379.

Beauchamp NJ, Makris M, Preston FE, Peake IR, Daly ME. 2000. Major structural defects in the antithrombin gene in four families with type I antithrombin deficiency—partial/complete deletions and rearrangement of the antithrombin gene. Thromb Haemost 83:715–721.

Beck CR, Collier P, Macfarlane C, Malig M, Kidd JM, Eichler EE, Badge RM, Moran JV. 2010. LINE-1 retrotransposition activity in human genomes. Cell 141:1159–1170.

Bertelsen B, Nazaryan-Petersen L, Sun W, Mehrjouy MM, Xie G, Chen W, Hjermind LE, Taschner PE, Tümer Z. 2015. A germline chromothripsis event stably segregating in 11 individuals through three generations. Genet Med.[Epub ahead of print], doi: 10.1038/gim.2015.112

Callinan PA, Wang J, Herke SW, Garber RK, Liang P, Batzer MA. 2005. Alu retrotransposition-mediated deletion. J Mol Biol 348:791–800.

Chen JM, Stenson PD, Cooper DN, Férec C. 2005. A systematic analysis of LINE-1 endonuclease-dependent retrotranspositional events causing human genetic disease. Hum Genet 117:411–427.

Chiang C, Jacobsen JC, Ernst C, Hanscom C, Heilbut A, Blumenthal I, Mills RE, Kirby A, Lindgren AM, Rudiger, SR, McLaughlan CJ, Bawden CS, et al. 2012. Complex reorganization and predominant non-homologous repair following chromosomal breakage in karyotypically balanced germline rearrangements and transgenic integration. Nat Genet 44:390–397.

Christensen SM, Eickbush TH. 2005. R2 target-primed reverse transcription: ordered cleavage and polymerization steps by protein subunits asymmetrically bound to the target DNA. Mol Cell 25:6617–6628.

Cost GJ. 2002. Human L1 element target-primed reverse transcription in vitro. EMBO J 21:5899–5910.

Crasta K, Ganem NJ, Dagher R, Lantermann AB, Ivanova EV, Pan Y, Nezi L, Protopopov A, Chowdhury D, Pellman D. 2012. DNA breaks and chromosome pulverization from errors in mitosis. Nature 482:53–58.

Deininger PL, Batzer MA. 1999. Alu repeats and human disease. Mol Genet Metab 67:183–193.

Dewannieux M, Esnault C, Heidmann T. 2003. LINE-mediated retrotransposition of marked Alu sequences. Nat Genet 35:41–48.

Elliott B, Richardson C, Jasin M. 2005. Chromosomal translocation mechanisms at intronic alu elements in mammalian cells. Mol Cell 17:885–894.

Ewing AD, Kazazian HH. 2010. High-throughput sequencing reveals extensive variation in human-specific L1 content in individual human genomes. Genome Res 20:1262–1270.

Ewing AD, Kazazian HH. 2011. Whole-genome resequencing allows detection of many rare LINE-1 insertion alleles in humans. Genome Res 21:985–990.

Feng Q, Moran JV, Kazazian HH, Boeke JD. 1996. Human L1 retrotransposon encodes a conserved endonuclease required for retrotransposition. Cell 87:905–916.

Garcia-Perez JL, Marchetto MCN, Muotri AR, Coufal NG, Gage FH, O'Shea KS, Moran JV. 2007. LINE-1 retrotransposition in human embryonic stem cells. Hum Mol Genet 16:1569–1577.

Gasior SL, Wakeman TP, Xu B, Deininger PL. 2006. The human LINE-1 retrotransposon creates DNA double-strand breaks. J Mol Biol 357:1383–1393.

Georgiou I, Noutsopoulos D, Dimitriadou E, Markopoulos G, Apergi A, Lazaros L, Vaxevanoglou T, Pantos K, Syrrou M, Tzavaras T. 2009. Retrotransposon RNA expression and evidence for retrotransposition events in human oocytes. Hum Mol Genet 18:1221–1228.

Gilbert N, Lutz-Prigge S, Moran JV. 2002. Genomic deletions created upon LINE-1 retrotransposition. Cell 110:315–325.

Gilbert N, Lutz S, Morrish TA, Moran JV. 2005. Multiple fates of L1 retrotransposition intermediates in cultured human cells. Mol Cell Biol 25:7780–7795.

Han K, Sen SK, Wang J, Callinan PA, Lee J, Cordaux R, Liang P, Batzer MA. 2005. Genomic rearrangements by LINE-1 insertion-mediated deletion in the human and chimpanzee lineages. Nucleic Acids Res 33:4040–4052.

Hancks DC, Goodier JL., Mandal PK, Cheung LE, Kazazian HH. 2011. Retrotransposition of marked SVA elements by human L1s in cultured cells. Hum Mol Genet 20:3386–3400.

Hancks DC, Kazazian HH. 2012. Active human retrotransposons: variation and disease. Curr Opin Genet Dev 22:191–203.

Helman E, Lawrence ML, Stewart C, Sougnez C, Getz G, Meyerson M. 2014. Somatic retrotransposition in human cancer revealed by whole-genome and exome sequencing. Genome Res 24:1053–1063.

Huang CRL, Schneider AM, Lu Y, Niranjan T, Shen P, Robinson MA, Steranka JP, Valle D, Civin CI, Wang T, Wheelan SJ, Ji H, et al. 2010. Mobile interspersed

repeats are major structural variants in the human genome. Cell 141:1171–1182.
Iskow RC, McCabe MT, Mills RE, Torene S, Pittard WS, Neuwald AF, Van Meir EG, Vertino PM, Devine SE. 2010. Natural mutagenesis of human genomes by endogenous retrotransposons. Cell 141:1253–1261.
Jalanko A, Manninen T, Peltonen L. 1995. Deletion of the C-terminal end of aspartylglucosaminidase resulting in a lysosomal accumulation disease: evidence for a unique genomic rearrangement. Hum Mol Genet 4:435–441.
Kajikawa M, Okada N. 2002. LINEs mobilize SINEs in the eel through a shared 3′ sequence. Cell 111:433–444.
Kano H, Godoy I, Courtney C, Vetter MR, Gerton GL, Ostertag EM, Kazazian HH. 2009. L1 retrotransposition occurs mainly in embryogenesis and creates somatic mosaicism. Genes Dev 23:1303–1312.
Kazazian HH Jr. 2004. Mobile elements: drivers of genome evolution. Science 303:1626–1632.
Kent WJ. 2002. BLAT-the BLAST-like alignment tool. Genome Res 12:656–664.
Kloosterman WP, Guryev V, van Roosmalen M, Duran KJ, de Bruijn E, Bakker SC, Letteboer T, van Nesselrooij B, Hochstenbach R, Poot M, Cuppen E. 2011a. Chromothripsis as a mechanism driving complex de novo structural rearrangements in the germline. Hum Mol Genet 20:1916–1924.
Kloosterman WP, Hoogstraat M, Paling O, Tavakoli-Yaraki M, Renkens I, Vermaat JS, van Roosmalen MJ, van Lieshout S, Nijman IJ, Roessingh W, van 't Slot R, van de Belt J, et al. 2011b. Chromothripsis is a common mechanism driving genomic rearrangements in primary and metastatic colorectal cancer. Genome Biol 12:R103.
Kloosterman WP, Tavakoli-Yaraki M, van Roosmalen MJ, van Binsbergen E, Renkens I, Duran K, Ballarati L, Vergult S, Giardino D, Hansson K, Ruivenkamp CA, Jager M, et al. 2012. Constitutional chromothripsis rearrangements involve clustered double-stranded DNA breaks and nonhomologous repair mechanisms. Cell Rep 1:648–655.
Kondo-Iida E, Kobayashi K, Watanabe M, Sasaki J, Kumagai T, Koide H, Saito K, Osawa M, Nakamura Y, Toda T. 1999. Novel mutations and genotype–phenotype relationships in 107 families with Fukuyama-type congenital muscular dystrophy (FCMD). Hum Mol Genet 8:2303–2309.
Kopera HC, Moldovan JB, Morrish TA, Garcia-Perez JL, Moran JV. 2011. Similarities between long interspersed element-1 (LINE-1) reverse transcriptase and telomerase. Proc Natl Acad Sci 108:20345–20350.
Kutsche K, Ressler B, Katzera HG, Orth U, Gillessen-Kaesbach G, Morlot S, Schwinger E, Gal A. 2002. Characterization of breakpoint sequences of five rearrangements in L1CAM and ABCD1 (ALD) genes. Hum Mutat 19:526–535.
Lee E, Iskow R, Yang L, Gokcumen O, Haseley P, Luquette LJ, Lohr JG, Harris CC, Ding L, Wilson RK, Wheeler DA, Gibbs RA, et al. 2012a. Landscape of somatic retrotransposition in human cancers. Science 337:967–971.
Lee J, Han K, Meyer TJ, Kim HS., Batzer MA. 2008. Chromosomal inversions between human and chimpanzee lineages caused by retrotransposons. PLoS One 3:e4047.
Lee J, Ha J, Son SY, Han K. 2012b. Human genomic deletions generated by SVA-associated events. Compar Funct Genom 2012:1–7.
Li L, Bray PF. 1993. Homologous recombination among three intragene Alu sequences causes an inversion-deletion resulting in the hereditary bleeding disorder Glanzmann thrombasthenia. Am J Hum Genet 53:140–149.
Li X, Heyer WD. 2008. Homologous recombination in DNA repair and DNA damage tolerance. Cell Res 18:99–113.
Lieber MR. 2010. The mechanism of double-strand DNA break repair by the nonhomologous DNA end-joining pathway. Annu Rev Biochem 79:181–211.
Liu P, Erez A, Nagamani SC, Dhar SU, Kołodziejska KE, Dharmadhikari AV, Cooper ML, Wiszniewska J, Zhang F, Withers MA, Bacino CA, Campos-Acevedo LD, et al. 2011. Chromosome catastrophes involve replication mechanisms generating complex genomic rearrangements. Cell 146:889–903.
Luan DD, Korman MH, Jakubczak JL, Eickbush TH. 1993. Reverse transcription of R2Bm RNA is primed by a nick at the chromosomal target site: a mechanism for non-LTR retrotransposition. Cell 72:595–605.
Malhotra A, Lindberg M, Faust GG, Leibowitz ML, Clark RA, Layer RM, Quinlan AR, Hall IM. 2013. Breakpoint profiling of 64 cancer genomes reveals numerous complex rearrangements spawned by homology-independent mechanisms. Genome Res 23:762–776.
Masson E, Hammel P, Garceau C, Bénech C, Quéméner-Redon S, Chen JM, Férec C. 2013. Characterization of two deletions of the CTRC locus. Mol Genet Metab 109:296–300.
Mathias SL, Scott AF, Kazazian HH, Boeke JD, Gabriel A. 1991. Reverse transcriptase encoded by a human transposable element. Science 254:1808–1810.
McVey M, Lee SE. 2008. MMEJ repair of double strand breaks (director's cut): deleted sequences and alternative endings. Trends Genet 24:529–538.
Mehine M, Mäkinen N, Heinonen HR, Aaltonen LA, Vahteristo P. 2014 Genomics of uterine leiomyomas: insights from high-throughput sequencing. Fertil Steril 102:621–629.
Miné M, Chen JM, Brivet M, Desguerre I, Marchant D, de Lonlay P, Bernard A, Férec C, Abitbol M, Ricquier D, Marsac C. 2007. A large genomic deletion in the PDHX gene caused by the retrotranspositional insertion of a full-length LINE-1 element. Hum Mutat 28:137–142.
Moran JV, Holmes SE, Naas TP, DeBerardinis RJ, Boeke JD, Kazazian HH. 1996. High frequency retrotransposition in cultured mammalian cells. Cell 87:917–927.
Morisada N, Rendtorff ND, Nozu K, Morishita T, Miyakawa T, Matsumoto T, Hisano S, Iijima K, Tranebjærg L, Shirahata A, Matsuo M, Kusuhara K. 2010. Branchio-otorenal syndrome caused by partial EYA1 deletion due to LINE-1 insertion. Pediatr Nephrol 25:1343–1348.
Narita N, Nishio H, Kitoh Y, Ishikawa Y, Ishikawa Y, Minami R, Nakamura H, Matsuo M. 1993. Insertion of a 5′ truncated L1 element into the 3′ end of exon 44 of the dystrophin gene resulted in skipping of the exon during splicing in a case of Duchenne muscular dystrophy. J Clin Invest 91:1862–1867.
Nazaryan L, Stefanou EG, Hansen C, Kosyakova N, Bak M, Sharkey FH, Mantziou T, Papanastasiou AD, Velissariou V, Liehr T, Syrrou M, Tommerup N. 2014 The strength of combined cytogenetic and mate-pair sequencing techniques illustrated by a germline chromothripsis rearrangement involving *FOXP2*. Eur J Hum Genet 22:338–343.
Okubo M, Horinishi A, Saito M, Ebara T, Endo Y, Kaku K, Murase T, Eto M. 2007. A novel complex deletion-insertion mutation mediated by Alu repetitive elements leads to lipoprotein lipase deficiency. Mol Genet Metab 92:229–233.
Ostertag EM, Goodier JL, Zhang Y, Kazazian HH. 2003. SVA elements are nonautonomous retrotransposons that cause disease in humans. Am J Hum Genet 73:1444–1451.
Ovchinnikov I, Troxel AB, Swergold GD. 2001. Genomic characterization of recent human LINE-1 insertions: evidence supporting random insertion. Genome Res 11:2050–2058.
Peixoto A, Pinheiro M, Massena L, Santos C, Pinto P, Rocha P, Pinto C, Teixeira MR. 2013. Genomic characterization of two large Alu-mediated rearrangements of the BRCA1 gene. J Hum Genet 58:78–83.
Raiz J, Damert A, Chira S, Held U, Klawitter S, Hamdorf M, Lower J, Stratling WH, Lower R, Schumann GG. 2012. The non-autonomous retrotransposon SVA is trans-mobilized by the human LINE-1 protein machinery. Nucleic Acids Res 40:1666–1683.
Schollen E, Keldermans L, Foulquier F, Briones P, Chabas A, Sánchez-Valverde F, Adamowicz M, Pronicka E, Wevers R, Matthijs G. 2007. Characterization of two unusual truncating PMM2 mutations in two CDG-Ia patients. Mol Genet Metab 90:408–413.
Segal Y, Peissel B, Renieri A, de Marchi M, Ballabio A, Pei Y, Zhou J. 1999. LINE-1 elements at the sites of molecular rearrangements in Alport syndrome-diffuse leiomyomatosis. Am J Hum Genet 64:62–69.
Sen SK, Han K, Wang J, Lee J, Wang H, Callinan PA, Dyer M, Cordaux R, Liang P, Batzer MA. 2006. Human genomic deletions mediated by recombination between Alu elements. Am J Hum Genet 79:41–53.
Shukla R, Upton KR, Muñoz-Lopez M, Gerhardt DJ, Fisher ME, Nguyen T, Brennan PM, Baillie JK, Collino A, Ghisletti S, Sinha S, Iannelli F, et al. 2014. Endogenous retrotransposition activates oncogenic pathways in hepatocellular carcinoma. Cell 153:101–111.
Solyom S, Ewing AD, Rahrmann EP, Doucet T, Nelson HH, Burns MB, Harris RS, Sigmon DF, Casella A, Erlanger B, Wheelan S, Upton KR, et al. 2012. Extensive somatic L1 retrotransposition in colorectal tumors. Genome Res 22:2328–2338.
Srikanta D, Sen SK, Conlin EM, Batzer MA. 2009. Internal priming: an opportunistic pathway for L1 and Alu retrotransposition in hominins. Gene 448:233–241.
Stephens PJ, Greenman CD, Fu B, Yang F, Bignell GR, Mudie LJ, Pleasance ED, Lau KW, Beare D, Stebbings LA, McLaren S, Lin ML, et al. 2011. Massive genomic rearrangement acquired in a single catastrophic event during cancer development. Cell 144:27–40.
Stewart C, Kural D, Strömberg MP, Walker JA, Konkel MK, Stütz AM, Urban AE, Grubert F, Lam HYK, Lee WP, Busby M, Indap AR, et al. 2011. A comprehensive map of mobile element insertion polymorphisms in humans. PLoS Genet 7:e1002236.
Su LK, Steinbach G, Sawyer JC, Hindi M, Ward PA, Lynch PM. 2000. Genomic rearrangements of the APC tumor-suppressor gene in familial adenomatous polyposis. Hum Genet 106:101–107.
Sukarova E, Dimovski AJ, Tchacarova P, Petkov GH, Efremov GD. 2001. An Alu insert as the cause of a severe form of hemophilia A. Acta Haematol 106:126–129.
Symer DE, Connelly C, Szak ST, Caputo EM, Cost GJ, Parmigiani G, Boeke JD. 2002. Human L1 retrotransposition is associated with genetic instability in vivo. Cell 110:327–338.
Takasu M, Hayashi R, Maruya E, Ota M, Imura K, Kougo K, Kobayashi C, Saji H, Ishikawa Y, Asai T, Tokunaga K. 2007. Deletion of entire HLA-A gene accompanied by an insertion of a retrotransposon. Tissue Antigens 70:144–150.
Tubio JMC, Li Y, Ju YS, Martincorena I, Cooke SL, Tojo M, Gundem G, Pipinikas CP, Zamora J, Raine K, Menzies A, Roman-Garcia P, et al. 2014. Extensive transduction of nonrepetitive DNA mediated by L1 retrotransposition in cancer genomes. Science 345:1251343–1251343.

Udaka T, Okamoto N, Aramaki M, Torii C, Kosaki R, Hosokai N, Hayakawa T, Takahata N, Takahashi T, Kosaki K. 2007. An Alu retrotransposition-mediated deletion of CHD7 in a patient with CHARGE syndrome. Am J Med Genet A 143A:721–726.

Untergrasser A, Cutcutache I, Koressaar T, Ye J, Faircloth BC, Remm M, Rozen SG. 2012. Primer3—new capabilities and interfaces. Nucleic Acids Res 40:e115.

van den Hurk JA, Meij IC, Seleme MC, Kano H, Nikopoulos K, Hoefsloot LH, Sistermans EA, de Wijs IJ, Mukhopadhyay A, Plomp AS, de Jong PT, Kazazian HH, et al. 2007. L1 retrotransposition can occur early in human embryonic development. Hum Mol Genet 16:1587–1592.

Vogt J, Bengesser K, Claes KB, Wimmer K, Mautner VF, van Minkelen R, Legius E, Brems H, Upadhyaya M, Hogel JH, Lazaro C, Rosenbaum T, et al. 2014. SVA retrotransposon insertion-associated deletion represents a novel mutational mechanism underlying large genomic copy number changes with non-recurrent breakpoints. Genome Biol 15:1–17.

Wang H, Xing J, Grover D, Hedges DJ, Han K, Walker JA, Batzer MA. 2005. SVA elements: a hominid-specific retroposon family. J Mol Biol 354:994–1007.

Wang T, Lerer I, Gueta Z, Sagi M, Kadouri L, Peretz T, Abeliovich D. 2001. A deletion/insertion mutation in the BRCA2 gene in a breast cancer family: a possible role of the Alu-polyA tail in the evolution of the deletion. Genes Chromosomes Cancer 31:91–95.

Witherspoon DJ, Xing J, Zhang Y, Watkins WS, Batzer MA, Jorde LB. 2010. Mobile element scanning (ME-Scan) by targeted high-throughput sequencing. BMC Genomics 11:410.

Xing J, Zhang Y, Han K, Salem AH, Sen SK, Huff CD, Zhou Q, Kirkness EF, Levy S, Batzer MA, Jorde LB. 2009. Mobile elements create structural variation: analysis of a complete human genome. Genome Res 19:1516–1526.

Zhang CZ, Spektor A, Cornils H, Francis JM, Jackson EK, Liu S, Meyerson M, Pellman D. 2015. Chromothripsis from DNA damage in micronuclei. Nature 522:179–184.

Zingler N, Willhoeft U, Brose HP, Schoder V, Jahns T, Hanschmann KM, Morrish TA, Lower J, Schumann GG. 2005. Analysis of 5'- junctions of human LINE-1 and Alu retrotransposons suggests an alternative model for 5'-end attachment requiring microhomology-mediated end-joining. Genome Res 15:780–789.